Nanotechnol. Environ. Eng. (2017) 2:5
https://doi.org/10.1007/s41204-017-0016-9

ORIGINAL PAPER

Effect of Fe_3O_4 nanoparticles on *Sphingobium yanoikuyae* XLDN2-5 cells in carbazole biodegradation

Huihui Sun[1] · Hanyue Ma[1] · Zhuang Liu[1] · Yufei Li[1] · Ping Xu[1] · Xia Wang[1]

Received: 13 March 2017 / Accepted: 17 April 2017 / Published online: 24 April 2017

Abstract This study explored the effect of Fe_3O_4 nanoparticles on *Sphingobium yanoikuyae* XLDN2-5, an important environmentally microorganism in carbazole biodegradation process. Microbial cell/Fe_3O_4 nanoparticles biocomposite was constructed by assembling Fe_3O_4 nanoparticles onto the surface of *Sphingobium yanoikuyae* XLDN2-5 cells. With the increase in Fe_3O_4 nanoparticles concentration, moderate deterioration in carbazole biodegradation was observed for microbial cell/Fe_3O_4 nanoparticles biocomposites. A concentration-dependent decrease in *Sphingobium yanoikuyae* XLDN2-5 viability caused by Fe_3O_4 nanoparticles was observed. Zeta potential measurements suggested that electrostatic repulsion between microbial cell and Fe_3O_4 nanoparticles reduced nanotoxicity at low Fe_3O_4 nanoparticles concentration. The morphology characterization showed the small size of Fe_3O_4 nanoparticle made it possible to penetrate *Sphingobium yanoikuyae* XLDN2-5 cell membrane. Furthermore, reactive oxygen species increases, membrane damage, and DNA damage should be responsible for the antibacterial mechanism of Fe_3O_4 nanoparticles at high concentration. This study presented essential knowledge for better understanding of Fe_3O_4 nanoparticles behavior in the environment, and helping to promote safer and more effective application of nanomaterials in nanotechnology-based environmental bioremediation.

Keywords Nanoparticles · Carbazole · Nanotoxicity · Bioremediation · Microbial cells

Introduction

Nanoscale iron particles represent a new generation of environmental remediation technologies that could provide cost-effective solutions to some of the most challenging environmental cleanup problems [35]. Due to biocompatibility, large surface areas, high surface reactivity, and superparamagentic properties, magnetic Fe_3O_4 nanoparticles are used widely for removing a broad range of environmental contaminants, such as gases [18], contaminated chemicals [17, 31], organic pollutants [12, 24, 25, 32], and biological substances [3]. Among these environmental applications, the immobilization of microorganisms using Fe_3O_4 nanoparticles has emerged as a novel aspect of the industrialization of microbial cell immobilization in environmental remediation [24, 25, 32]. Different types of microbial cells (bacteria, yeasts, algae) were modified to prepare the biocomposites of microbial cells and nanomaterials [22]. For example, microbial cells of *Pseudomonas delafieldii* R-8 coated with nanoparticles were used as biocatalysts in biodesulfurization [24, 25]. Magnetically modified *Saccharomyces* and *Kluyveromyces* cells were used for the adsorption of water soluble dyes from water solutions [20, 21]. Because of increasing production and application of Fe_3O_4 nanoparticles, their release into the environment would be inevitable, which requires a better understanding of their behavior and interaction with microorganisms in the environment. Nevertheless, current studies in environmental remediation are mostly focused on the removing of environmental contaminants, the immobilization of microorganisms using Fe_3O_4

Huihui Sun and Hanyue Ma have contributed equally to this work.

✉ Xia Wang
ghwx@sdu.edu.cn

[1] State Key Laboratory of Microbial Technology, Shandong University, Jinan 250100, People's Republic of China

nanoparticles, and the activity of immobilized microbial cells, while rarely on the understanding of interaction mechanism with microorganisms and potential of antibacterial activities associated with Fe_3O_4 nanoparticles.

The interaction mechanism and cytotoxicity of Fe_3O_4 nanoparticles vary depending on the nature of the target microorganisms [7]. *Sphingobium yanoikuyae* XLDN2-5 is an important representative of environmentally microorganisms used for bioremediation of toxic compounds such as carbazole [4, 16]. In our previous studies, the immobilization of this strain was obtained successfully by encapsulating *Sphingobium yanoikuyae* XLDN2-5 cells in the mixture of Fe_3O_4 nanoparticles and gellan gum [31] and assembling Fe_3O_4 nanoparticles onto the surface of *Sphingobium yanoikuyae* XLDN2-5 cells [13]. The resulting immobilized *Sphingobium yanoikuyae* XLDN2-5 cells exhibited good biodegradation activity and reusability at low Fe_3O_4 nanoparticles concentration, but low biodegradation activity at high Fe_3O_4 nanoparticles concentration. Based on our previous studies, the effect of Fe_3O_4 nanoparticles on *Sphingobium yanoikuyae* XLDN2-5 cell in carbazole biodegradation process will be further explored in this study, which will give us some insights on how Fe_3O_4 nanoparticles pose the potential negative effect in the environment and microbial ecosystem.

This study focused on the antibacterial activity and interaction mechanism with *Sphingobium yanoikuyae* XLDN2-5 cell associated with Fe_3O_4 nanoparticles in carbazole biodegradation. Microbial cell/Fe_3O_4 nanoparticle biocomposites were constructed by assembling different concentrations of Fe_3O_4 nanoparticles onto the surface of *Sphingobium yanoikuyae* XLDN2-5 cells in this study. The morphologies of Fe_3O_4 nanoparticles and microbial cell/Fe_3O_4 nanoparticle biocomposites were verified by a transmission electronic microscopy. The biodagradation activities of the resulted microbial cell/Fe_3O_4 nanoparticles biocomposites were compared. Additionally, the antibacterial activity and interaction mechanism between Fe_3O_4 nanoparticles and *Sphingobium yanoikuyae* XLDN2-5 cells were also analyzed by toxicity assessment, zeta (ζ) potential measurement, reactive oxygen species test, cell wall/membrane damage assay, and confocal microscopy.

Materials and methods

Chemicals and nanomaterials

Carbazole was purchased from Sigma-Aldrich (St. Louis. MO). Fe_3O_4 nanoparticles were prepared by the coprecipitation method with some modifications as described before [31]. All other chemicals were of analytical grade and commercially available.

To prepare nanoparticles suspensions, an appropriate amount Fe_3O_4 nanoparticles was added to distilled water. After ultrasonic disruption (25 kHz, 10 min; BUG25-06, BRANSON, USA), the suspensions were prepared for microbial cell/nanoparticle biocomposites construction and TEM detection.

Microorganism and cultivation

The model organism used in this study was *Sphingobium yanoikuyae* XLDN2-5 (gram-negative), which can use carbazole as the sole source of carbon, nitrogen, and energy, was cultivated in the mineral salts medium (MSM) as previously described [4]. Microbial cells were harvested in the exponential phase (the optical density was about 0.68–0.70 at 620 nm) of growth by centrifugation at $6000\times g$ for 10 min as previously described [31]. The pellet was washed twice with distilled water to eliminate complicating effects associated with macromolecules and other constituents in culture media and then resuspended in distilled water to achieve an initial concentration of 0.1 g/mL before used.

Construction of microbial cell/Fe_3O_4 nanoparticle biocomposites

In the construction of microbial cell/Fe_3O_4 nanoparticle biocomposites experiments, microbial cells suspension and Fe_3O_4 nanoparticles suspension were mixed with the ratio of the wet mass of microbial cells to the dry mass of Fe_3O_4 nanoparticles being approximately 1:1, 1:2, 1:3, 1:4, and 1:5. The mixtures were fully mixed by vortexing and then incubated for 2 h at 30 °C in a dark shaker to obtain microbial cell/Fe_3O_4 nanoparticle biocomposites.

Biodegradation experiments

The biodegradation performances of different microbial cell/Fe_3O_4 nanoparticle biocomposites described above were tested with the same initial content of carbazole at the same incubation conditions. All biodegradation experiments were carried out in 100-mL flasks containing 10 mL MSM at 30 °C on a reciprocal shaker at 180 rpm. In each experiment, 3500 μg of carbazole was added to MSM, and microbial cell/Fe_3O_4 nanoparticle biocomposites served as biocatalysts. Additionally, the same amount of microbial cells (cell wet weight was 50 mg) was conducted in all batch biodegradation as control. All experiments were performed in triplicate.

Nanotoxicity assessment

The microbial cells suspension was diluted to 2×10^8 CFU/mL (colony forming units, CFU) with a sterile saline solution (0.85% w/v, NaCl in distilled water)

for Fe_3O_4 nanoparticles exposure treatment. For the exposure experiment, 5 mL microbial cells suspension was added to a 100-mL flask. Then, 5 mL Fe_3O_4 nanoparticles suspension was added to achieve Fe_3O_4 nanoparticles exposure concentration of 5, 10, 15, 20, and 25 g/L, respectively. After incubation for 2 h at 30 °C on a reciprocal shaker at 180 rpm, the mixtures were diluted serially and plated on Luria–Bertani (LB) agar plates. The plates were cultivated at 30 °C for 24 h. The toxicity of Fe_3O_4 nanoparticles was evaluated by comparing the number of CFU with the control after 24-h incubation at 30 °C [8]. The mixture containing microbial cells suspension and sterile saline solution (0.85% w/v, NaCl in distilled water) instead of Fe_3O_4 nanoparticles suspension was used as control. All experiments were repeated at least three times to ensure data repeatability.

Zeta potential measurement

Zeta potentials of all samples were measured by a Zetasizer (Malvern Instruments Ltd., USA) at 25 °C to deduce surface charge. Fe_3O_4 nanoparticles suspension and microbial cell suspension were diluted to 1×10^{-3} g/L and 0.1×10^{-2} g/L by sterile deionized water (pH 7.2), respectively. The samples were put into an ultrasound bath for 30 min to disperse aggregates before the zeta potential measurement.

Reactive oxygen species test

Intracellular reactive oxygen species (ROS) in *Sphingobium yanoikuyae* XLDN2-5 cells were measured using dichlorofluorescein diacetate (DCFH-DA, Yeasen) as described by Lyon et al. [14] with minor modifications. Microbial cells culture was collected by centrifugation at $6000 \times g$ for 10 min. The pellet was resuspended with sterile saline solution (0.85% w/v, NaCl in distilled water) to 2×10^5 CFU/mL and stained with DCFH-DA dye (0.1 μM) for 20 min in darkness. Then, the microbial cells were washed twice using phosphate-buffered saline (PBS, pH 7.4, 10 mM) to remove excess fluorescent dye. Fe_3O_4 nanoparticles concentrations tested were 1, 10, 20, 50, and 100 mg/mL, respectively. Then, 500 μL nanoparticles suspension and 500 μL microbial cells suspension were mixed in Eppendorf tube for 2 h at 30 °C in a dark shaker. Finally, the fluorescence values were measured at an excitation wavelength of 485 nm and emission wavelength of 528 nm in a 96-well plate using a Victor^{3TM} multiwell plate reader (Perkin Elmer).

Membrane damage assay

Sphingobium yanoikuyae XLDN2-5 cell membrane integrity was evaluated using a standard, fluorescence-based, and nucleic acid assay. Both free microbial cells (2×10^5 CFU/mL) and microbial cell/Fe_3O_4 nanoparticle biocomposites obtained by incubating microbial cells with Fe_3O_4 nanoparticles (1, 10, 20, 100 mg/mL; 2 h at 30 °C) were stained with propidium iodide (PI, 2 μM, Sigma) for 20 min in dark and then washed twice in PBS (pH 7.0, 10 mM) to remove excess fluorescent dye. The percentage of inactivated cells was determined by the ratio of microbial cells stained with PI using BD FACSCalibur flow cytometry (488 nm excitation, 525 nm emission).

Analytical methods

After each batch of biodegradation, 20 mL anhydrous ethanol was added to the biodegradation mixture, followed by centrifugation (12,000 rpm for 10 min) and filtration through a 0.22-um filter. Residual contents of carbazole were determined using high-performance liquid chromatography (HPLC). HPLC performed with an Agilent 1100 series (Hewlett-Packard) instrument equipped with a reversed-phase C18 column (4.6 mm × 150 mm, Hewlett-Packard). The mobile phase was a mixture of methanol and deionized water (90:10, v/v) at a flow rate of 0.5 mL/min, and carbazole was monitored at 254 nm with a variable-wavelength detector.

The size and morphology of Fe_3O_4 nanoparticles and microbial cell/Fe_3O_4 nanoparticle biocomposites were determined by transmission electronic microscope (JEM-100cx II, JEOL, Japan). Each sample was prepared by evaporating a drop of properly diluted nanoparticles suspension on a carbon copper grid.

The DNA damage was determined by a confocal microscope (LSM700, Zeiss, Germany). *Sphingobium yanoikuyae* XLDN2-5 cells suspension (1 mg/mL) incubated with Fe_3O_4 nanoparticles (5 mg/mL) were served as experimental group. Free microbial cells served as control. Free microbial cells and microbial cells treated with Fe_3O_4 nanoparticles were fixed on a slide, treated with methanol, and stained with 4′,6-diamidino-2-phenylindole (DAPI) to visualize the DNA fragmentation using a confocal microscope (LSM700, Zeiss, Germany).

Results and discussion

Effect of Fe_3O_4 nanoparticle on carbazole biodegradation at different conditions

Due to unique physicochemical properties, magnetic Fe_3O_4 nanoparticles are used widely in environmental remediation. In our previous study, microbial cell/Fe_3O_4 nanoparticle biocomposite was constructed by assembling Fe_3O_4 nanoparticles onto the surface of *Sphingobium yanoikuyae* XLDN2-5 cells [13]. Further, the resulting microbial cell/Fe_3O_4 nanoparticle biocomposite exhibited good carbazole biodegradation activity and reusability compared with free cells [13]. Recently, the negative effect of nanomaterials was paid close attention [5, 9, 10, 15, 34]. Considering this, the microbial cell/Fe_3O_4 nanoparticle biocomposites were constructed at different ratios of Fe_3O_4 nanoparticles to microbial cells. Then, the carbazole biodegradation performances of the resulted microbial cell/Fe_3O_4 nanoparticle biocomposite were evaluated as shown in Fig. 1a. The results showed that the highest carbazole biodegradation activity was presented by free microbial cells and microbial cell/Fe_3O_4 nanoparticle biocomposite at the ratio of the dry mass of Fe_3O_4 nanoparticles to the wet mass of cells being 1:1 (w/w), and 3500 μg carbazole could be degraded completely in 7 h. However, the carbazole biodegradation activities of the microbial cell/Fe_3O_4 nanoparticle biocomposites significantly decreased with the increase in Fe_3O_4 nanoparticles concentration. The equivalent amount of carbazole could be degraded slowly in 9 h by the microbial cell/Fe_3O_4 nanoparticle biocomposite at the ratio of 1:2 (w/w). Only 16% carbazole was degraded in 9 h at the ratio of 1:3 (w/w). In contrast, almost no carbazole biodegradation was observed for the microbial cell/Fe_3O_4 biocomposites at the ratio from 1:4 to 1:5 (w/w). This may be that the nanotoxicity of Fe_3O_4 nanoparticles to *Sphingobium yanoikuyae* XLDN2-5 cells increased with the increase in Fe_3O_4 nanoparticles concentration, which would, in turn, decrease the carbazole biodegradation performances of the microbial cell/Fe_3O_4 nanoparticle biocomposites.

Viability of microbial cells after exposure to Fe_3O_4 nanoparticles

In view of the adverse effect of Fe_3O_4 nanoparticles on the carbazole biodegradation performances of *Sphingobium yanoikuyae* XLDN2-5 cells, the antibacterial properties of Fe_3O_4 nanoparticles were investigated by conventional plate count method. Culturability data of *Sphingobium yanoikuyae* XLDN2-5 cells after exposure to Fe_3O_4 nanoparticles for 2 h are shown in Fig. 1b. A dose-dependent reduction in culturability was observed for *Sphingobium yanoikuyae* XLDN2-5 cells after exposure to Fe_3O_4 nanoparticles for 2 h. At the ratio of Fe_3O_4 nanoparticles to microbial cells being 1:1 (w/w), *Sphingobium yanoikuyae* XLDN2-5 cells showed about 25% of lethality rate, which was consistent with that the microbial cell/Fe_3O_4 nanoparticle biocomposite exhibited the same biodegradation activity as free cells as shown in Fig. 1a. These results indicated that *Sphingobium yanoikuyae* XLDN2-5 cells showed limited resistance to Fe_3O_4 nanoparticles at low concentration as described in previous studies [19, 28, 29]. However, Fe_3O_4 nanoparticles presented relatively high nanotoxicity to *Sphingobium yanoikuyae* XLDN2-5 cells at higher Fe_3O_4 nanoparticles concentration. When the ratio increased to 1:4 and 1:5 (w/w), the lethality rates of *Sphingobium yanoikuyae* XLDN2-5 cells after exposure to Fe_3O_4 nanoparticles for 2 h were

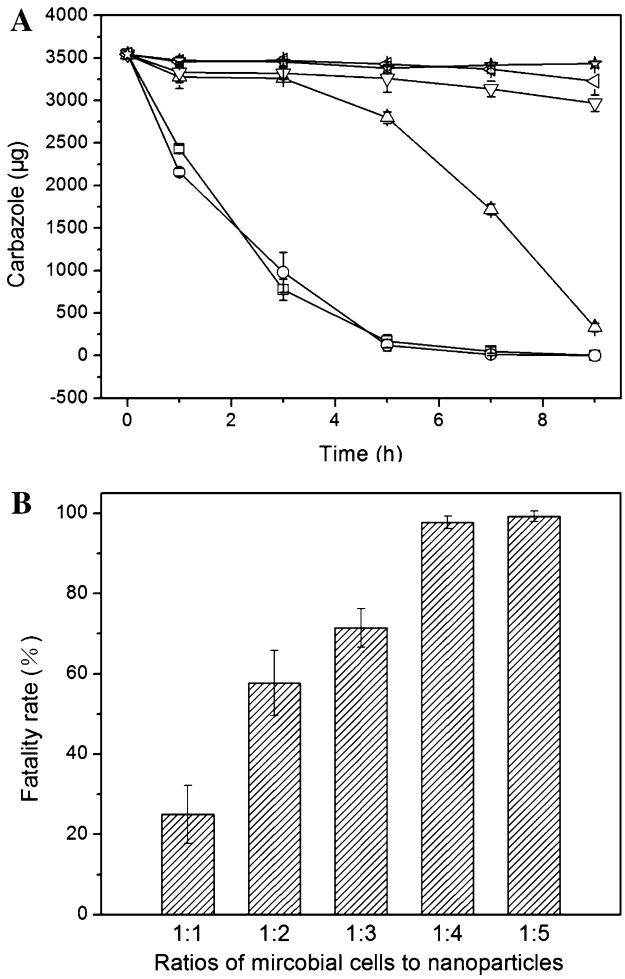

Fig. 1 **a** Carbazole biodegradation by microbial cell/Fe_3O_4 nanoparticle biocomposites. Control (*open square*); ratios of 1:1 (*open circle*), 1:2 (*triangle*), 1:3 (*inverted triangle*), 1:4 (*left triangle*), and 1:5 (*star*); **b** microbial cell viability after exposure to Fe_3O_4 nanoparticles measured by conventional plate count method

98 and 99%, respectively (Fig. 1b), indicating almost completely lethal of *Sphingobium yanoikuyae* XLDN2-5 cells.

Zeta potential measurement

Electrostatic interaction between nanoparticles and bacteria were believed to contribute to nanoparticles binding to cell membrane, membrane interference, and reduce cell viability [23]. The surface charges of Fe_3O_4 nanoparticle and *Sphingobium yanoikuyae* XLDN2-5 cell were detected as shown in Table 1. The zeta (ζ) potential of Fe_3O_4 nanoparticle was -22.9 mV at pH 7.2. The surface charge of *Sphingobium yanoikuyae* XLDN2-5 cell was -8.49 mV measured at the same condition. The zeta potential measurements suggested that there was a high degree of electrostatic repulsion between the negatively charged Fe_3O_4 nanoparticles and the negatively charged *Sphingobium yanoikuyae* XLDN2-5 cells. This formed an electrostatic barrier between *Sphingobium yanoikuyae* XLDN2-5 and Fe_3O_4 nanoparticles, which could reduce the nanotoxicity for *Sphingobium yanoikuyae* XLDN2-5 cell at low Fe_3O_4 nanoparticles concentration [2].

Characterization of nanoparticles and microbial cells/nanoparticle biocomposite

Small size of nanoparticles may partially contribute to their antibacterial activity [1, 9, 33]. In order to understand the microbial cell's response to nanoparticles stress, changes in bacterial morphology were examined using TEM. The morphology and size of Fe_3O_4 nanoparticles were determined by TEM as shown in Fig. 2a. The average particle size of Fe_3O_4 nanoparticles was about 20 nm, which made it possible for Fe_3O_4 nanoparticles to penetrate the microbial cell membrane, which could lead to ROS generation, DNA damage, and ultimately cell death. Figure 2b showed *Sphingobium yanoikuyae* XLDN2-5 cell coated with Fe_3O_4 nanoparticles at 1:1 (w/w) ratio. Moreover, Fe_3O_4 nanoparticles were efficiently assembled on the surface of *Sphingobium yanoikuyae* XLDN2-5 cell due to the large specific surface area and high surface energy of nanoparticles. Furthermore, some smaller size particles distributed inside *Sphingobium yanoikuyae* XLDN2-5 cell,

Table 1 Zeta potential of Fe_3O_4 nanomaterials and *Sphingobium yanoikuyae* XLDN2-5

Nanomaterials or microbial cells	ζ potential (mV)
Sphingobium yanoikuyae XLDN2-5 cells	-8.49 ± 2.54
Fe_3O_4 nanoparticles	-22.9 ± 0.61

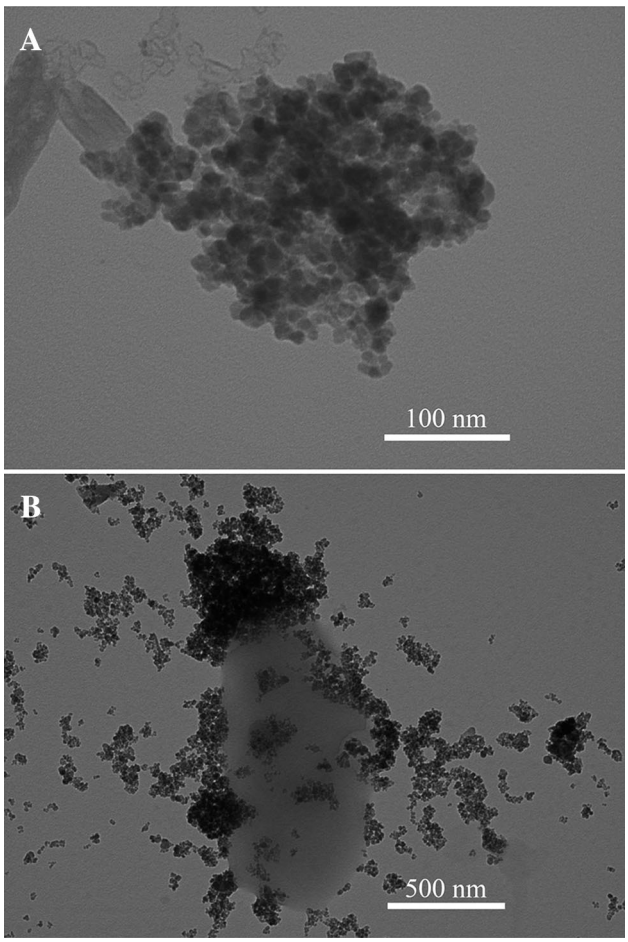

Fig. 2 **a** TEM images of Fe_3O_4 nanoparticles and **b** *Sphingobium yanoikuyae* XLDN2-5 coated with Fe_3O_4 nanoparticles

which is consistent with previous study that indicated bio-uptake of TiO_2 nanoparticles by electron microscopic observations [9], suggesting a toxicity mechanism for physical attachment and uptake.

Effect of Fe_3O_4 nanoparticles on intracellular ROS level

Oxidative stress triggered by ROS generation was generally considered to be responsible for the antibacterial activity of nanoparticles [27, 30]. The generation of ROS was evaluated to determine whether it was involved in the concentration-dependent nanotoxicity of Fe_3O_4 nanoparticles. To elucidate the dark mechanism of Fe_3O_4 nanoparticles toxicity, the effect of Fe_3O_4 nanoparticles exposure on cellular ROS level was probed using DCFH-DA staining as shown in Fig. 3a. After 2 h of exposure to Fe_3O_4 nanoparticles, Fe_3O_4 induced a drastic increase in ROS intracellular level in *Sphingobium yanoikuyae* XLDN2-5 compared with control. Additionally, ROS detection results demonstrated a dose-dependent increase in the formation

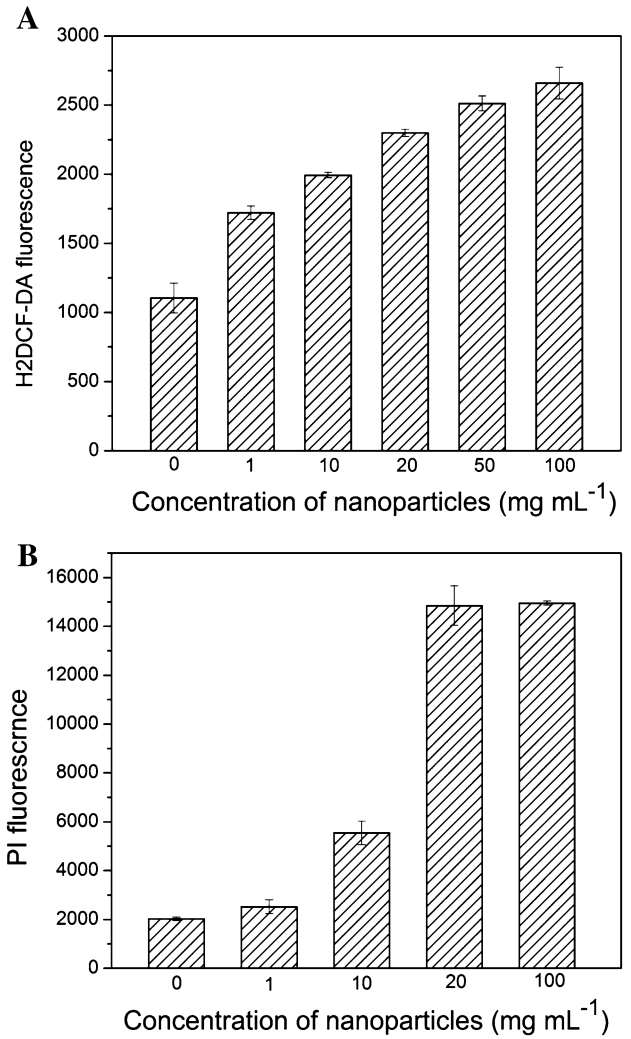

Fig. 3 **a** Intracellular ROS level after exposure to Fe_3O_4 nanoparticles at different concentrations; **b** fluorescence-based microbial cell viability assay associated with membrane damage

of ROS as shown in Fig. 3a, which indicated that the higher exposure concentration induced a drastic increase in intracellular ROS level in *Sphingobium yanoikuyae* XLDN2-5 cells.

Membrane damage assay

It was reported that bacterial cell wall is designed to provide strength, rigidity, and shape, and to protect the bacterial cell from osmotic rupture and mechanical damage [26], which plays an important role in tolerance or susceptibility of bacteria to nanoparticles. Thus, membrane damage assays are a strong surrogate for *Sphingobium yanoikuyae* XLDN2-5 cell death. In this study, membrane damage was evaluated via a fluorescent staining method as shown in Fig. 3b. A concentration-dependent significant increase in fluorescence intensity was observed in treated *Sphingobium yanoikuyae* XLDN2-5 cells compared to control, showing an increase in membrane permeability. At low exposure concentration, Fe_3O_4 nanoparticles exhibited relatively weak membrane damage. By increasing the concentration of Fe_3O_4 nanoparticles to 100 mg/mL[1], the membrane damage was significantly increased. *Sphingobium yanoikuyae* XLDN2-5 was a gram-negative bacterium [4]. One distinct feature of gram-negative bacteria is the presence of lipopolysaccharide (LPS) layer, which contributes greatly to the structural integrity of the bacteria and protects the cell from a variety of toxic molecules compared to gram-positive bacteria [6]. It is clear that membrane damage could be an important factor that promoted the cell death at higher Fe_3O_4 nanoparticles. Furthermore, the accumulation of Fe_3O_4 nanoparticles on the surface of Fe_3O_4 nanoparticles cell, as shown in Fig. 2b, may contribute to the disruption of cell membrane due to a significant increase in permeability [11].

Confocal fluorescence microscopy imaging

To further investigate whether DNA damage was a result of exposure to Fe_3O_4 nanoparticles, *Sphingobium yanoikuyae* XLDN2-5 cells after exposure to Fe_3O_4 nanoparticles for 2 h at 30 °C were tested for double-strand breaks (DSBS) in DNA by a confocal microscopy. Figure 4b shows slight nuclear fragmentation was observed in *Sphingobium yanoikuyae* XLDN2-5 cells after exposure with 5 mg/mL Fe_3O_4 nanoparticles compared to control (Fig. 4a). These results showed that Fe_3O_4 nanoparticles possess evident DNA-damaging potential in *Sphingobium yanoikuyae* XLDN2-5 cells confirmed by confocal microscopy, which may be attributed to the increase in oxidative stress caused by internalized Fe_3O_4 nanoparticles. These results also further verified the ROS generation and membrane damage results as shown in Fig. 3.

Conclusions

In conclusion, the interaction mechanism and cytotoxicity of Fe_3O_4 nanoparticles against *Sphingobium yanoikuyae* XLDN2-5 were evaluated as a novel aspect in upcoming nanotechnology-based environmental engineering. As an important representative of environmentally microorganisms used for carbazole bioremediation, the carbazole biodegradation activities of *Sphingobium yanoikuyae* XLDN2-5 cell/Fe_3O_4 nanoparticle biocomposites significantly decreased with the increase in Fe_3O_4 nanoparticles concentration. This was considered to be due to the dose-dependent increase in nanotoxicity presented by Fe_3O_4 nanoparticles. The zeta (ζ) potential suggested that electrostatic repulsion existed between *Sphingobium*

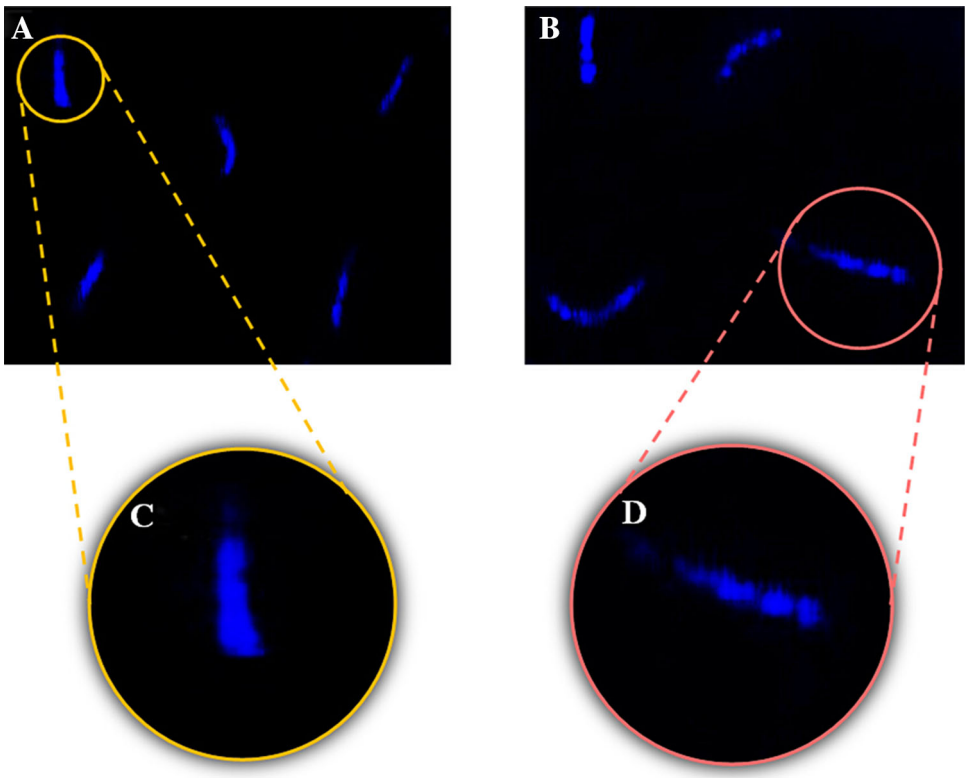

Fig. 4 Confocal microphotographs (DAPI stained) showing DNA fragmentation in microbial cells treated with Fe_3O_4 nanoparticles. **a** Control; **b** microbial cells after exposed to 5 mg/mL Fe_3O_4 nanoparticles. **c**, **d** Enlargements of **a** and **b**, respectively

yanoikuyae XLDN2-5 cells and Fe_3O_4 nanoparticles, which reduced the toxicity of Fe_3O_4 nanoparticles at low concentration. Small size made it possible for Fe_3O_4 nanoparticles to penetrate *Sphingobium yanoikuyae* XLDN2-5 cell membrane. ROS generation with a concomitant membrane damage and DNA damage contributed to the death of *Sphingobium yanoikuyae* XLDN2-5 cells. These results provided essential knowledge for better understanding of Fe_3O_4 nanoparticles behavior in the environment, helping to promote safer and more effective application of nanomaterials in upcoming nanotechnology-based environmental bioremediation.

Funding Funding was provided by National Natural Science Foundation of China (Grant Nos. 31570103, 21177074).

References

1. Agnihotri S, Mukherji S, Mukherji S (2014) Size-controlled silver nanoparticles synthesized over the range 5–100 nm using the same protocol and their antibacterial efficacy. RSC Adv 4:3974–3983
2. Badawy AME, Silva RG, Morris B, Scecke KG, Suidan MT, Tolaymat TM (2011) Surface charge-dependent toxicity of silver nanoparticles. Environ Sci Technol 45:283–287
3. Bosetti M, Massè A, Tobin E, Cannas M (2002) Silver coated materials for external fixation devices: in vitro biocompatibility and genotoxicity. Biomaterials 23:887–892
4. Gai ZH, Yu B, Li L, Wang Y, Ma C, Feng J, Deng Z, Xu P (2007) Cometabolic degradation of dibenzofuran and dibenzothiophene by a newly isolated carbazole-degrading *Sphingomonas* sp. strain. Appl Environ Microbiol 73:2832–2838
5. Gajjar P, Brian P, David WB, Huang WJ, Johnson WP, Anderson AJ (2009) Antimicrobial activities of commercial nanoparticles against an environmental soil microbe, *Pseudomonas putida* KT2440. J Biol Eng 3:9–22
6. Guine V, Spadini L, Sarret G, Muris M, Delolme C, Gaudet JP, Martins JMF (2006) Zinc sorption to three gram-negative bacteria: combined titration, modeling, and EXAFS study. Environ Sci Technol 40:1806–1813
7. Hajipour MJ, Fromm KM, Ashkarran AK, Aberasturi DJ, Larramendi IR, Rojo T, Serpooshan V, Parak WJ, Mahmoudi M (2012) Antibacterial properties of nanoparticles. Trends Biotechnol 30:499–511
8. Jiang W, Mashayekhi H, Xing B (2009) Bacterial toxicity comparison between nano- and micro-scaled oxide particles. Environ Pollut 157:1619–1625
9. Kumar A, Pandey AK, Singh SS, Shanker R, Dhawan A (2011) Engineered ZnO and TiO_2 nanoparticles induce oxidative stress and DNA damage leading to reduced viability of *Escherichia coli*. Free Radical Bio Med 51:1872–1881
10. Kumari J, Kumar D, Mathur A, Naseer A, Kumar RR (2014) Cytotoxicity of TiO_2 nanoparticles towards freshwater sediment microorganisms at low exposure concentrations. Environ Res 135:333–345
11. Kaweeteerawat C, Ivask A, Liu R, Zhang HY, Chang CH, Low-Kam C, Fischer H, Ji ZX, Pokhrel S, Cohen Y, Telesca D, Zink J, Mädler L, Holden PA, Nel A, Godwin H (2015) Toxicity of metal oxide nanoparticles in *Escherichia coli* correlates with conduction band and hydration energies. Environ Sci Technol 49:1105–1112
12. Lein H, Zhang W (2001) Nanoscale iron particles for complete reduction of chlorinated ethenes. Colloids Surface A 191:97–105

13. Li YF, Du XY, Wu C, Liu XY, Wang X, Xu P (2013) An efficient magnetically modified microbial cell biocomposite for carbazole biodegradation. Nanoscale Res Lett 8:522–526
14. Lyon DY, Brunet L, Hinkal GW, Wiesner MR, Alvarez PJJ (2008) Antibacterial activity of fullerene water suspensions (nC60) is not due to ROS-mediated damage. Nano Lett 8:1539–1543
15. Maurer-Jones MA, Gunsolus IL, Murphy CJ, Haynes CL (2013) Toxicity of engineered nanoparticles in the environment. Anal Chem 85:3036–3049
16. Ouchiyama N, Zhang Y, Omori T, Kodama T (1993) Biodegradation of carbazole by *Pseudomonas* spp. CA06 and CA10. Biosci Biotechnol Biochem 57:455–460
17. Ponder SM, Darab JG, Mallouk TE (2000) Remediation of Cr(VI) and Pb(II) aqueous solutions using supported nanoscale zero-valent iron. Environ Sci Technol 34:2564–2569
18. Rodriguez JA (2006) The chemical properties of bimetallic surfaces: importance of ensemble and electronic effects in the adsorption of sulfur and SO_2. Prog Surf Sci 81:141–189
19. Sadiq IM, Chowdhury B, Chandrasekaran N, Mukherjee A (2009) Antimicrobial sensitivity of *Escherichia coli* to alumina nanoparticles. Nanomed Nanotechnol 5:282–286
20. Safarikova M, Ptackova L, Kibrikova I, Safarik I (2005) Biosorption of water-soluble dyes on magnetically modified *Saccharomyces cerevisiae* sub sp. uvarum cells. Chemosphere 59:831–835
21. Safarik I, Ptackova L, Safarikova M (2002) Adsorption of dyes on magnetically labeled baker's yeast cells. Eur Cells Mater 3:52–55
22. Safarik I, Safarikova M (2007) Magnetically modified microbial cells: a new type of magnetic adsorbents. China Particuol 5:19–25
23. Seil JT, Webeter TJ (2012) Antimicrobial application of nanotechnology: methods and literature. Int J Nanomed 7:2767–2781
24. Shan GB, Zhang HY, Cai WQ, Xing JM, Liu HZ (2005) Improvement of biodesulfurization rate by assembling nanosorbents on the surface of microbial cells. Biophys J 89:L58–L60
25. Shan GB, Xing JM, Zhang HY, Liu HZ (2005) Biodesulfurization of dibenzothiophene by microbial cells coated with magnetic nanoparticles. Appl Environ Microbiol 71:4497–4502
26. Singleton P (2014) Bacteria in biology, biotechnology and medicine, 6th edn. Wiley, West Sussex, ISBN 0-470-09027-8:570
27. Subbiahdoss G, Sharifi S, Grijpma DW, Laurent S, van der Mei HC, Mahmoudi M, Busscher HJ (2012) Magnetic targeting of surface-modified superparamagnetic iron oxide nanoparticles yields antibacterial efficacy against biofilms of gentamicin-resistant staphylococci. Acta Biomater 8:2047–2055
28. Taylor EN, Webster TJ (2009) The use of super paramagnetic nanoparticles for prosthetic biofilm prevention. Int J Nanomed 4:145–152
29. Tran N, Mir A, Mallik D, Sinha A, Nayar S, Webster TJ (2010) Bactericidal effect of iron oxide nanoparticles on *Staphylococcus aureus*. Int J Nanomed 5:277–283
30. Von Moos N, Slaveykova VI (2014) Oxidative stress induced by inorganic nanoparticles in bacteria and aquatic microalgae-state of the art and knowledge gaps. Nanotoxicology 8:605–630
31. Wang X, Gai ZH, Yu B, Feng JH, Xu CY, Yuan Y, Xin LJ, Xu P (2007) Degradation of carbazole by microbial cells immobilized in magnetic gellan gum gel beads. Appl Environ Microbiol 73:6421–6428
32. Xu P, Yu B, Li LF, Cai FX, Ma CQ (2006) Microbial degradation of sulfur, nitrogen and oxygen heterocycles. Trends Microbiol 14:398–405
33. Xu L, Weiner BM, Kleckner N (1997) Meiotic cells monitor the status of the interhomolog recombination complex. Genes Dev 11:106–118
34. You J, Zhang YY, Hu ZQ (2011) Bacteria and bacteriophage inactivation by silver and zinc oxide nanoparticles. Colloids Surf B 85:161–167
35. Zhang WX (2003) Nanoscale iorn particles for environmental remediation: an overview. J Nanopart Res 5:323–332